THE DEVELOPMENTAL BASIS OF EVOLUTIONARY CHANGES IN LIMB PROPORTIONS

BY

CATHERINE DALTON HUGHES

THESIS

Submitted in partial fulfillment of the requirements
for the degree of Master of Science in Biology
with a concentration in Ecology, Ethology, and Evolution
in the Graduate College of the
University of Illinois at Urbana-Champaign, 2015

Urbana, Illinois

Master's Committee:

Assistant Professor Karen Sears, Director of Research
Research Assistant Professor Jonathan Marcot
Professor Emeritus Jo Ann Cameron

ABSTRACT

Mammalian limbs are complex morphological structures that exhibit an astonishing amount of diversity. This diversity is driven by changes in the relative proportions of the three limb segments that are conserved among mammals. Despite the importance of limb proportions to mammalian evolution, the developmental mechanisms that regulate mammalian limb proportions remain largely unknown. In this study, I address three questions whose answers will provide insights into the mechanisms through which mammalian segment proportion is determined: when and how does the forelimb achieve its adult proportions, when and how does the hind limb achieve its adult proportions, and when and how does the proportions of the fore- and hind limb diverge. I address these questions using mouse, the model mammalian species. Results of this study indicate that adult forelimb segment proportions are achieved through differing rates of segment growth after their initial condensation, adult hind limb segment proportions are achieved through differing rates of growth after their initial condensations, and fore- and hind limb proportions diverge by the time of the initial cartilage condensation of segments. These findings suggest that the proportions of mammalian limb segments are not established until well after their cartilage condensation, and sets up future research on the specific cellular and molecular mechanisms driving proportion differences among species.

TABLE OF CONTENTS

INTRODUCTION……...……1

METHODS……..……4

RESULTS……7

DISCUSSION……..9

REFERENCES……..12

FIGURES……...14

INTRODUCTION

Mammalian limbs are complex morphological structures that exhibit an astonishing amount of diversity (Polly 2007). The diversity is achieved in part through modifications in the relative proportions of the three segments that all mammals possess along the proximal-distal axis of the limb: the stylopod (S), zeugopod (Z), and autopod (A) corresponding to the humerus/femur, radius-ulna/tibia-fibula, and carpels/tarsals respectively (Polly, 2007; Radinsky, 1987; Young & Hallgrímsson, 2005; Young, 2013). Because of this, we must understand the mechanisms by which mammalian segment proportions are achieved before we can fully comprehend the factors that have shaped mammalian evolution. As a first step toward this goal, I investigated when adult limb proportions are achieved during mammalian development, using the mouse, *Mus musculus*, as a model organism. Specifically, I explored when mouse fore- and hind limbs achieve their adult proportions, and when the proportions of mouse fore- and hind limbs diverge from one another.

The developmental mechanisms that regulate mammalian limb proportions are largely undetermined (Sanger et al., 2011) in part because the developmental mechanisms that control segmentation along the limb's proximal-distal axis remain unresolved. Numerous models have been proposed to explain limb segmentation along the proximal-distal (PD) axis through developmental time. The two most accepted of these models are the Progress Zone Model and the Inhibitory Cascade Model. According to the Progress Zone Model, limb segmentation occurs via an autonomous clock in which undifferentiated mesenchymal cells acquire positional information based on time spent in a progress—zone region (Galloway, Delgado, Ros, & Tabin, 2009; Summerbell, Lewis, & Wolpert, 1973). In theory, cells spending more time in the progress-zone are exposed to higher levels of fibroblast growth factor (FGF) signals from the apical ectodermal region (AER), which leads to them developing more distal characteristics (autopod-like) (Tabin & Wolpert, 2007). This model was originally supported by experiments in which the AER was removed from the developing chick limb. If the AER is removed early in limb development, the result is a truncated limb in which only the stylopod is present (Saunders, 1998; Summerbell et al., 1973).

In contrast to the Progress Zone Model, the Inhibitory Cascade Model posits that signals from the distal (FGF) and proximal (retinoic acid – RA) limb work in conjunction to pattern the

limb's proximal-distal axis. FGF and RA act antagonistically to set up a morphogen gradient (Mercader et al., 2000; Young, Winslow, Takkellapati, & Kavanagh, 2015). Cells exposed to high levels of RA and low levels of FGF form proximal segments, while cells exposed to low levels of RA and high levels of FGF produce distal segments (Cooper et al., 2011; Torres, 2011). Most recent studies support the Inhibitory Cascade Model over the Progress Zone Model (Young et al., 2015).

The most recent, and perhaps only, model for how limb segment proportions are determined is also based on the hypothesis that opposing molecular signals regulate segment formation. In this case, researchers have proposed that a self-organizing reaction-diffusion mechanism determines segment proportions, in which a locally diffusible, activator of segment condensation (e.g. TGF-b) and a laterally acting inhibitor (e.g. FGF) antagonistically interact (Newman & Müller, 2005; Young, 2013). This model predicts that the zeugopod should occupy approximately 1/3 of total limb length, with the stylopod and autopod together comprising the other 2/3. As a result, this model predicts that as stylopod length increases autopod length should decrease, and vice versa. However, this model only holds for adult proportions if later segment growth does not overwhelm the signal produced during segment determination (Sanger et al., 2011; Sears, Behringer, Rasweiler, & Niswander, 2006). Furthermore, there is no experimental evidence that causally links putative activators and inhibitors of segment condensation (Newman & Müller, 2005). Nevertheless, this model is supported by the finding that the zeugopod does tend to comprise approximately 1/3 of total limb length in adult mammals (Fischer & Blickhan, 2006; Schmidt & Fischer, 2009; Sears, Behringer, Rasweiler, & Niswander, 2007; Young & Hallgrímsson, 2005; Young, 2013).

In this study, I address three questions whose answers will provide insights into the mechanisms through which mammalian segment proportion is determined: when and how does the forelimb achieve its adult proportions, when and how does the hind limb achieve its adult proportions, and when and how does the proportions of the fore-and hind limb diverge. Adult limb segment proportions could be achieved at several time points during development: they could be achieved at the onset of mesenchymal condensation, at the onset of cartilage condensation, at the time of ossification, or at some point thereafter. Each of these findings would have different implications for the developmental mechanisms that drive the relative proportions of limb segments. For example, if I find that segment proportions are determined by

the onset of cartilage condensation, then this would suggest that developmental processes acting before the onset of condensation regulate limb segment proportions. This finding would support the activator-inhibitor model of limb segment specification described above. In contrast, if I find that adult segment proportions are not established until much later in development, then this would suggest that any proportion signals caused by an activator-inhibitor model are likely overwhelmed by later developmental processes.

METHODS

I first measured adult limb proportions of skeletal preparations and quantified the proportions relative to the entire limb. I then collected mouse embryos ranging from E9.5 to E16.5 and performed both *in situ* hybridizations and Alcian staining to visualize pre-cartilage and cartilage limb segmentation. Measurements were then taken from microscope images and used for statistical analyses against the adult proportional data.

Specimens – Skeletons of adult ICR mice (N=25 females, 23 males) from the Sears Lab collection were used in this study. To prepare these skeletons, bodies of adult mice were obtained from the Sears Lab breeding colony and skeletonized using the Sears Lab dermestids. All use of the Sears Lab breeding colony was performed in accordance with University of Illinois Institutional Animal Care and Use Committee Guidelines (IACUC).

Mouse embryos from developmental stages E9.5 to E16.5 (Wanek, Muneoka, Holler-Dinsmore, Burton, & Bryant, 1989) (ADD IN THEILER) were also collected from Sears Lab breeding colony. Embryos were collected at every half-day during this range. A male and female mouse were placed in a breeding cage overnight and checked for the presence of vaginal plugs each morning. If found the mating was predicted to have taken place a midnight the previous day. Embryos were used for Whole Mount *In Situ* Hybridization (WISH) and Alcian staining protocol. All embryos were fixed in 4% paraformaldehyde (PFA) overnight at 4^{o}C, then dehydrated through a methanol series and stored at -20^{o}C until use. For all experiments, limbs were dissected off and staged using published staging guides (Wanek et al., 1989). The earliest limbs used in this study were from the bud stage of development, and the latest were fully formed limbs with all skeletal elements present.

Whole Mount *In situ* hybridization (WISH) – WISH was performed on embryos ranging in age from E9.5 to E13.5 for a transcription factor in the Sox (SRY-related high mobility group) box protein family, *Sox9* (Liao 2014). *Sox9* visualizes the pre-cartilage condensations of the developing limb segments. The WISH protocol I used was adapted from Maier et al. 2013 and spanned a four-day period. Day 1 consisted of sequential washes including bleaching in 6% hydrogen peroxide/methanol for one hour, a forty-minute methanol series,

repeated rinses in PBT, various time intervals in a proteinase K treatment (depending on the embryonic stage), a PBT rinse, fixative rinse in a 4% paraformaldehyde and 0.02% gluteraldehdye in PBT solution, and final PBT rinses. Day 1 concluded with a one-hour incubation in pre-hybridization solution in a 70^{o} oven and overnight in both pre-hybridization and probe solution. Day 2 began with five separate rinses in solution 1 at 70^{o}, continued in a mixed solution of solution1:MABT for one hour, then blocking for one hour each in both blocking solution 1 (2% blocking reagent/MABT) and 2 (20% heat inactivated goat serum/2% BR/MABT). Day 2 concluded with an overnight incubation in a 4^{o} cold room in blocking solution 2 with added anti-DIG antibody at a concentration of 1:2000. Day 3 consisted of six washes of MABT in one-hour time intervals with the sixth wash occurring overnight in the 4^{o} cold room. Day 4 was devoted to color development in each embryonic limb. Embryos were washed in NTMT four times for ten minutes each and submerged in BM-purple solution (Roche) and kept in the dark until appropriate gene expression was observed. All individual limbs were then photographed and kept in a 1% PFA solution for long-term storage at 4^{o} C.

Alcian staining – Alcian blue staining was used to visualize cartilaginous segments of the developing limb from E13 to 16.5 in half-day intervals (McLeod, 1980). Distinct and quantifiable cartilage condensations appear beginning at E13 and endochondral ossification begins at E16 (Hall & Miyake, 2000). Fore- and hind limbs were dissected off embryos. Limbs were rehydrated through a methanol series before washing in PBS for 30 minutes. Subsequently, limbs were submerged in an Alcian blue solution overnight (0.02% Alcian blue in ethanol and 30% glacial acetic acid). The following day limbs were washed in 100%, 95%, and 70% ethanol respectively for an hour and then washed for one house in deionized water. Limbs were then cleared in a 1% KOH solution and changed everyday until skeletal features were visible. Finished samples were placed in a 2:1 KOH/Glycerol solution for storage (Cooper et al., 2014). All individual limbs were then photographed.

Limb segmentation measurements – *Embryonic*. Alcian stained limbs were imaged using a Leica DFC425 Digital Color Microscope Camera and Leica Application Suite V3.8.0 imaging software. Images were then measured using ImageJ 1.48v software (NIH). Each segment (stylopod/zeugopod/digit) was measured three independent times, recorded and an

average was calculated. Measurements were categorized into developmental stages and forelimb versus hind limb.

Adult - Measurements were performed using calipers and each segment (stylopod/zeugopod/autopod) was measured three independent times, recorded, and an average was calculated.

Statistics – *Fore- and hind limb proportions*. I analyzed and compared the growth rates of each segment. To do this I first log-transformed the length values, then regressed the length of segments on the overall length of the limb, and then calculated the slope in JMP. This slope represents the growth rate of the segment, with a greater slope indicating a greater growth rate. I limited my analyses to embryonic days 14.5 and greater, as limb segment proportions are relatively stable prior to this timepoint. I also quantified the limb segment proportions in adult mice, and compared the proportions of the fore and hind limb across individuals using a series of non-parametric Wilcoxon tests.

RESULTS

When and how does the forelimb achieve its adult proportions?

Unfortunately, *Sox9* WISH never visualized all three limb segments in a single specimen (Figure 1) and therefore could not be used to quantify relative segment proportions. The remainder of this study will therefore focus on the results from the Alcian staining on E13 to E16.5 mice (Figure 2).

In adult mice, the zeugopod occupies the biggest proportion of the length of the forelimb at 46%, followed by the stylopod at 36%, and then the autopod at 18%. At the earliest stage in which all forelimb segments could be visualized using Alcian blue (E13), the stylopod makes up the biggest proportion of the length of the forelimb (39%), followed by the autopod (32%) and then the zeugopod (29%). The proportion of the forelimb comprising the stylopod remains relatively constant throughout prenatal development (ranges from 36 to 40%), while the proportion comprising the zeugopod dramatically increases (29 to 46%), and the proportions comprising the autopod dramatically decreases (32 to 18%) (Figure 3). The 95% confidence interval for the slope (rate of growth) of each segment does not overlap with the slopes of any other segments: Stylopod, Slope = 0.362, St Error of Slope = 0.0207, 95% Confidence Interval = 0.321 to 0.403, Zeugopod, Slope = 0.425, St Error of Slope = 0.0178, 95% Confidence Interval = 0.389 to 0.461, Autopod, Slope = 0.213, St Error of Slope = 0.0370, 95% Confidence Interval = 0.139 to 0.287 (Figure 4). This suggests that the rates of growth of all segments differ at a statistically significant level.

When and how does the hind limb achieve its adult proportions?

In adult mice, the zeugopod occupies the largest proportion of the length of the hind limb at 41%, followed by the stylopod at 32%, and the autopod at 27%. At the earliest stage in which all hind limb segments could be visualized using Alcian staining (E13), the stylopod and autopod comprise comparable proportions of the hind limb (35% and 36%, respectively), and the zeugopod a smaller proportion (29%). The proportions of the limb segments appear to be relatively stable through embryonic day 14. As hind limb development generally lags forelimb development by 0.5 to 1 day, this corresponds to embryonic day 13 to 13.5 in the forelimb. After embryonic day 14, the proportion of the hind limb comprising the stylopod remains relatively

constant (36%), the proportion comprising the zeugopod dramatically increases (from 28% to 41%), and the proportion comprising the autopod dramatically decreases (from 36% to 25%) (Figure 5). The 95% confidence interval for the slope (rate of growth) of the autopod overlaps with that of the stylopod, but the 95% confidence interval for the slope of the zeugopod does not overlap the slopes of any other segments: Stylopod, Slope = 0.933, St Error of Slope = 0.0704, 95% Confidence Interval = 0.792 to 1.074, Zeugopod, Slope = 1.270, St Error of Slope = 0.0860, 95% Confidence Interval = 1.098 to 1.442, Autopod, Slope = 0.783, St Error of Slope = 0.1697, 95% Confidence Interval = 0.444 to 1.122 (Figure 6). This suggests that the growth rate of the zeugopod significantly differs from that of the other segments.

How and when do the proportions of the fore- and hind limbs diverge?

The average proportions for the segments of the adult forelimb are 36% for the stylopod, 46% for the zeugopod, and 18% for the autopod. The average proportions for the segments of the adult hind limb are 32% for the stylopod, 41% for the zeugopod, and 27% for the autopod. Based on these numbers, the stylopod and zeugopod are relatively shorter in the hind than the forelimb, and the autopod is relatively longer. Statistical tests indicate that these differences in limb proportions between the fore- and hind limb are significant: Stylopod forelimb vs. Stylopod hind limb, ChiSquare = 69.90, DF = 1, $P < 0.001$*, Zeugopod forelimb vs. zeugopod hind limb, ChiSquare = 71.26, DF = 1, $P < 0.001$*, Autopod forelimb vs autopod hind limb, ChiSquare = 71.01, DF = 1, $P < 0.001$* (Figure 7). These results suggest that the proportions of all segments significantly differ in mouse fore- and hind limbs (Figure 8).

To investigate when these differences arise during development, I compared the proportion of the limb occupied by a segment in the fore versus the hind limb beginning at the first timepoint in which all segments could be visualized with Alcian staining (E13). The stylopod of the forelimb (39%) is already relatively longer than that of the hind limb (35%) by the earliest timepoint investigated (E13). At E13, the zeugopod of the fore- and hind limb have comparable relative lengths (29% and 29%, respectively), but the zeugopod of the forelimb is relatively longer by the next investigated stage (31% for the forelimb versus 29% for the hind limb) (E13.5).

DISCUSSION

An understanding of the mechanisms underlying limb segment proportions has not yet been achieved, but is vital to a comprehensive understanding of how vertebrate limb evolution occurred and continues to shape mammalian diversity of Earth (Sanger et al., 2011). In this study, I investigated the development of segment proportions in the model mammalian organism, mouse.

Adult forelimb segment proportions are achieved through differing rates of segment growth after their initial condensation. This study documented an increase in the relative length of the zeugopod and decrease in the relative length of the autopod throughout development. Results of this study also suggest that this change in relative segment proportions is driven by a slower rate of growth in the autopod and faster rate in the zeugopod after initial segment condensation. In addition, the rate of growth of the autopod appears to dramatically slow after embryonic day 16 (Figures 3 and 4). Taken together, these finding suggest that the adult segment proportions of mouse forelimbs are not achieved until well after their initial condensation, and likely through differential rates of segment growth.

Adult hind limb segment proportions are achieved through differing rates of growth after their initial condensations. This study also documented an increase in the relative proportion of the limb comprising the zeugopod and an associated decrease in the relative proportion comprising the autopod in the mouse hind limb during its development. Results further suggest that this change in segment proportions is driven by a higher rate of growth in the zeugopod after initial segment condensation (Figures 5 and 6). Similar to the findings for the mouse forelimb, findings for the mouse hind limb also suggest that the adult segment proportions of mouse hind limbs are not achieved until well after their initial cartilage condensation, and likely through differential rates of segment growth.

Fore- and hind limb proportions diverge by the time of the initial cartilage condensation of segments. Results of this study indicate that the significant differences in segment proportions between adult fore- and hind limbs are established relatively early in

development. Specifically, results suggest that the differences in proportions of the stylopod and autopod are likely established at or before E13 (the time at which all three segments have formed cartilage condensations) and that of the zeugopod by E13.5. This suggests that the processes driving these differences in proportions occur before or at the time of cartilage condensation.

Recently, researchers proposed a model for how the proportions of limb segments are achieved (Young et al., 2015; Young, 2013). This model proposes that proportions of adult limbs are the result of antagonistic interactions between activating and inhibiting signals during initial segment condensation (Young et al., 2015; Young, 2013). This model predicts that the zeugopod should comprise 1/3 of total limb length, with the stylopod and autopod together comprising the other 2/3. As a result, this model predicts that as stylopod length increases autopod length should decrease, and vice versa. In support of this model, studies of adult mammals have demonstrated that the zeugopod generally comprises 1/3 of the length of both fore- and hind limb (Schilling & Petrovitch, 2006). However, the results of this study suggest that the zeugopod occupies more than 1/3 of total limb length throughout pre-natal development. In addition, results of this study suggest that adult limb proportions are not achieved until after cartilage condensation, which is well after the time in which segments are established in the activator-inhibitor model. Studies in other systems also suggest that adult limb proportions are not achieved until later in development (Sanger et al., 2011; Schilling & Petrovitch, 2006; Sears et al., 2006). The early divergence time of the fore- and hind limb proportions observed in this study does suggest that developmental processes acting at or before segment condensations can impact adult segment proportions. However, taken as a whole the results of this study suggest that these early signals are largely overwhelmed by differences in the later growth of segment proportions (Sanger et al., 2011; Schmidt & Fischer, 2009; Young, 2013). Therefore, this study does not support the activator-inhibitor model for limb segment proportions.

Future Directions – This study provides fundamental information for understating when adult proportions become set up embryonically in mouse. There are four primary hypotheses for how proportions are achieved: (1) there is a difference in the number of cells before mesenchymal condensation, (2) there is a difference in the rate of cellular proliferation in segments, (3) there is a difference in the timing of segment differentiation, and (4) there is a difference in the elongation of each segment after cartilage condensation. Results from this study

suggest that the fore- and hind limb proportions are not established until after cartilage condensation, which provides support for the fourth of these hypotheses. Future study is needed to determine the cellular and molecular mechanisms by which the differential elongation of segments is achieved.

REFERENCES

Cooper, K. L., Hu, J. K.-H., ten Berge, D., Fernandez-Teran, M., Ros, M. a, & Tabin, C. J. (2011). Initiation of proximal-distal patterning in the vertebrate limb by signals and growth. *Science (New York, N.Y.)*, *332*(6033), 1083–1086. http://doi.org/10.1126/science.1199499

Cooper, K. L., Sears, K. E., Uygur, A., Maier, J., Baczkowski, K., Brosnahan, M., … Tabin, C. J. (2014). Patterning and post-patterning modes of evolutionary digit loss in mammals. *Nature*, *511*(7507), 41–45. http://doi.org/10.1038/nature13496

Fischer, M. S., & Blickhan, R. (2006). The tri-segmented limbs of therian mammals: Kinematics, dynamics, and self-stabilization - A review. *Journal of Experimental Zoology Part A: Comparative Experimental Biology*. http://doi.org/10.1002/jez.a.333

Galloway, J. L., Delgado, I., Ros, M. a, & Tabin, C. J. (2009). A reevaluation of X-irradiation-induced phocomelia and proximodistal limb patterning. *Nature*, *460*(7253), 400–404. http://doi.org/10.1016/j.ydbio.2009.05.532

Hall, B. K., & Miyake, T. (2000). All for one and one for all: Condensations and the initiation of skeletal development. *BioEssays*, *22*(2), 138–147. http://doi.org/10.1002/(SICI)1521-1878(200002)22:2<138::AID-BIES5>3.0.CO;2-4

McLeod, M. J. (1980). Differential staining of cartilage and bone in whole mouse fetuses by alcian blue and alizarin red S. *Teratology*, *22*(3), 299–301. http://doi.org/10.1002/tera.1420220306

Mercader, N., Leonardo, E., Piedra, M. E., Martínez-A, C., Ros, M. a, & Torres, M. (2000). Opposing RA and FGF signals control proximodistal vertebrate limb development through regulation of Meis genes. *Development (Cambridge, England)*, *127*(18), 3961–3970. http://doi.org/Opposing RA and FGF signals control proximodistal vertebrate limb development through regulation of Meis genes

Newman, S. a., & Müller, G. B. (2005). Origination and innovation in the vertebrate limb skeleton: An epigenetic perspective. *Journal of Experimental Zoology Part B: Molecular and Developmental Evolution*, *304*(6), 593–609. http://doi.org/10.1002/jez.b.21066

Polly, P.D. 2007. Limbs in mammalian evolution. Pp. 245-268. Fins into limbs: evolution, development, and transformation. University of Chicago Press, Chicago.

Radinsky. (1987). Diversity of mammalian design. Pp. 151-162. The evolution of vertebrate design. University of Chicago Press, Chicago.

Sanger, T. J., Norgard, E. a., Pletscher, L. S., Bevilacqua, M., Brooks, V. R., Sandell, L. J., & Cheverud, J. M. (2011). Developmental and genetic origins of murine long bone length variation. *Journal of Experimental Zoology Part B: Molecular and Developmental Evolution*, *316 B*(2), 146–161. http://doi.org/10.1002/jez.b.21388

Saunders, J. W. (1998). The proximo-distal sequence of origin of the parts of the chick wing and the role of the ectoderm. 1948. *The Journal of Experimental Zoology*, *282*(6), 628–668. http://doi.org/10.1002/jez.1401080304

Schilling, N., & Petrovitch, A. (2006). Postnatal allometry of the skeleton in Tupaia glis (Scandentia: Tupaiidae) and Galea musteloides (Rodentia: Caviidae) - A test of the three-segment limb hypothesis. *Zoology*, *109*(2), 148–163. http://doi.org/10.1016/j.zool.2005.11.004

Schmidt, M., & Fischer, M. S. (2009). Morphological integration in mammalian limb proportions: Dissociation between function and development. *Evolution*, *63*(3), 749–766. http://doi.org/10.1111/j.1558-5646.2008.00583.x

Sears, K. E., Behringer, R. R., Rasweiler, J. J., & Niswander, L. a. (2006). Development of bat flight: morphologic and molecular evolution of bat wing digits. *Proceedings of the National Academy of Sciences of the United States of America*, *103*(17), 6581–6586. http://doi.org/10.1073/pnas.0509716103

Sears, K. E., Behringer, R. R., Rasweiler, J. J., & Niswander, L. a. (2007). The evolutionary and developmental basis of parallel reduction in mammalian zeugopod elements. *The American Naturalist*, *169*(1), 105–117. http://doi.org/10.1086/510259

Summerbell, D., Lewis, J. H., & Wolpert, L. (1973). Positional information in chick limb morphogenesis. *Nature*, *244*(5417), 492–496. http://doi.org/10.1038/244492a0

Tabin, C., & Wolpert, L. (2007). Rethinking the proximodistal axis of the vertebrate limb in the molecular era. *Genes and Development*, *21*(12), 1433–1442. http://doi.org/10.1101/gad.1547407

Torres, M. (2011). Proximodistal Limb Subdivision. *Science*, (May), 1086–1088.

Wanek, N., Muneoka, K., Holler-Dinsmore, G., Burton, R., & Bryant, S. V. (1989). A staging system for mouse limb development. *The Journal of Experimental Zoology*, *249*(1), 41–49. http://doi.org/10.1002/jez.1402490109

Young, N. M. (2013). Macroevolutionary diversity of amniote limb proportions predicted by developmental interactions. *Journal of Experimental Zoology Part B: Molecular and Developmental Evolution*, *320*(7), 420–427. http://doi.org/10.1002/jez.b.22516

Young, N. M., & Hallgrímsson, B. (2005). Serial homology and the evolution of mammalian limb covariation structure. *Evolution; International Journal of Organic Evolution*, *59*(12), 2691–2704. http://doi.org/10.1111/j.0014-3820.2005.tb00980.x

Young, N. M., Winslow, B., Takkellapati, S., & Kavanagh, K. (2015). Shared rules of development predict patterns of evolution in vertebrate segmentation. *Nature Communications*, *6*, 6690. http://doi.org/10.1038/ncomms7690

FIGURES

Figure 1. *Sox9* expression in mouse from E9.5 to E13.5.

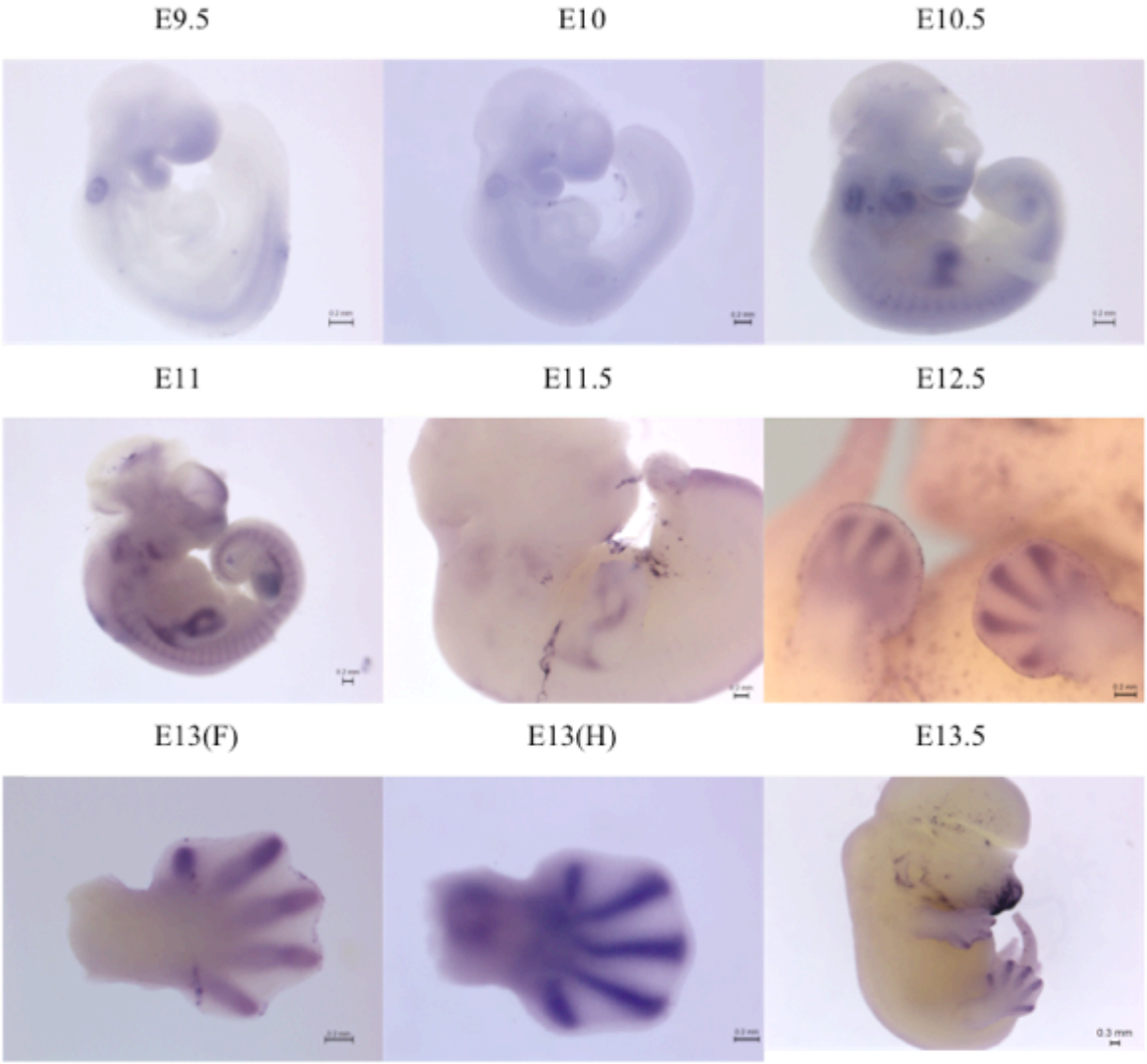

Figure 2. Alcian Staining of Cartilage from E13 to E16.5.

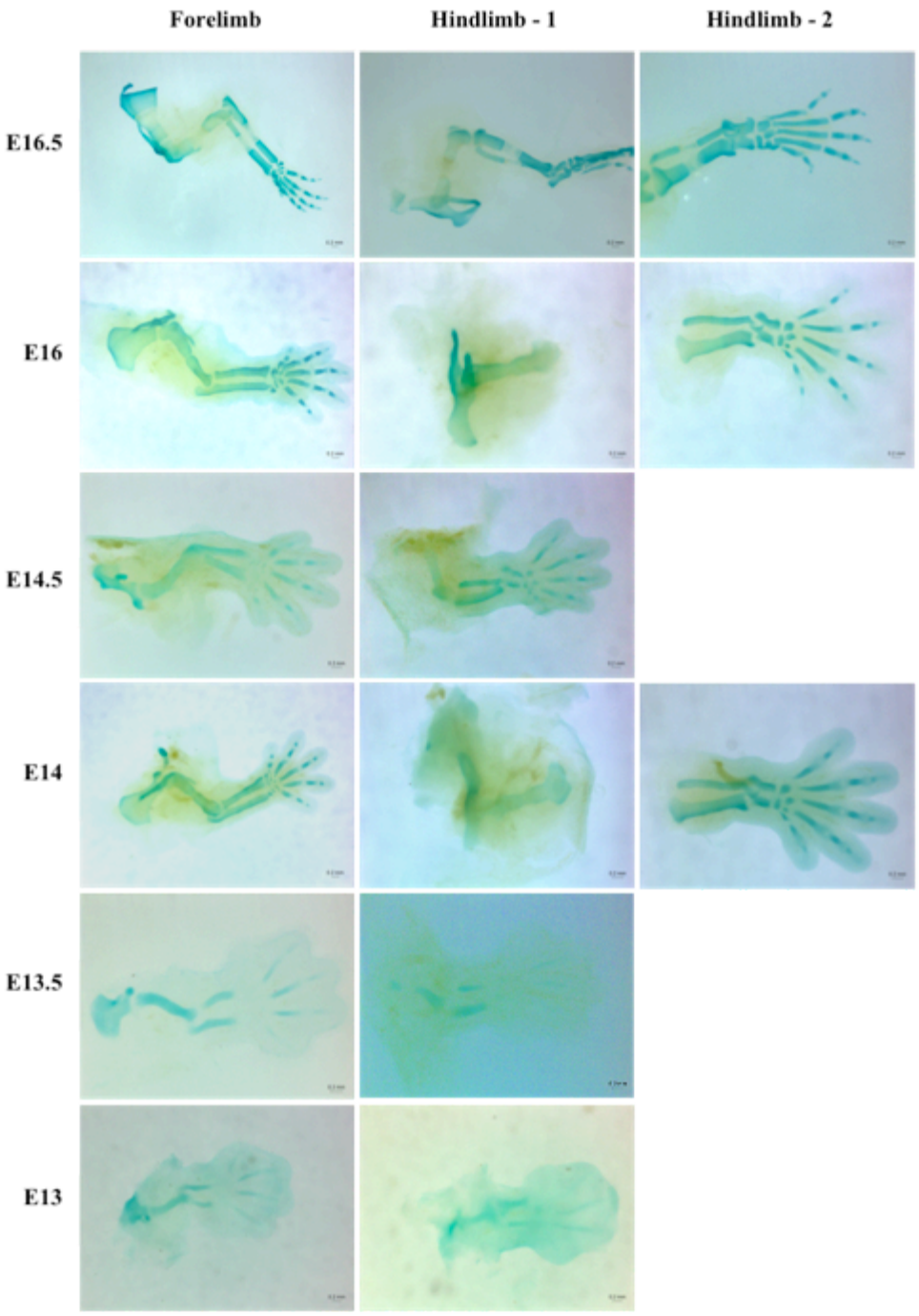

Figure 3. Relative segment length in forelimb throughout development.

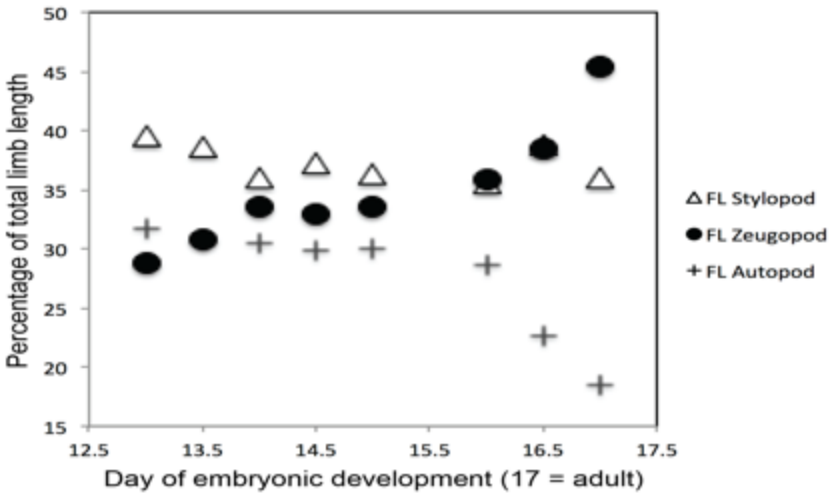

Figure 4. Growth rate of segments in forelimb throughout development.

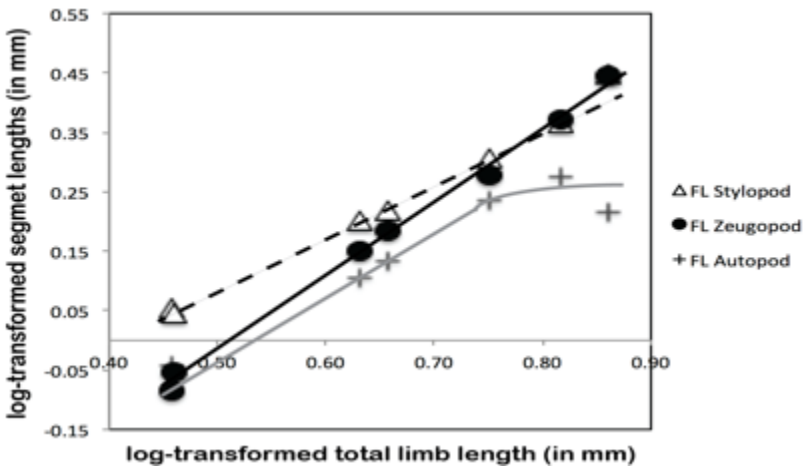

Figure 5. Relative segment length in hind limb throughout development.

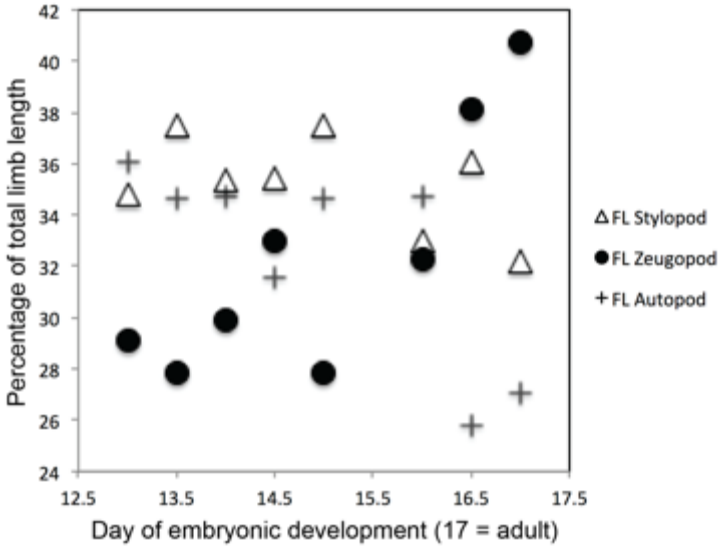

Figure 6. Growth rate of segments in hind limb throughout development.

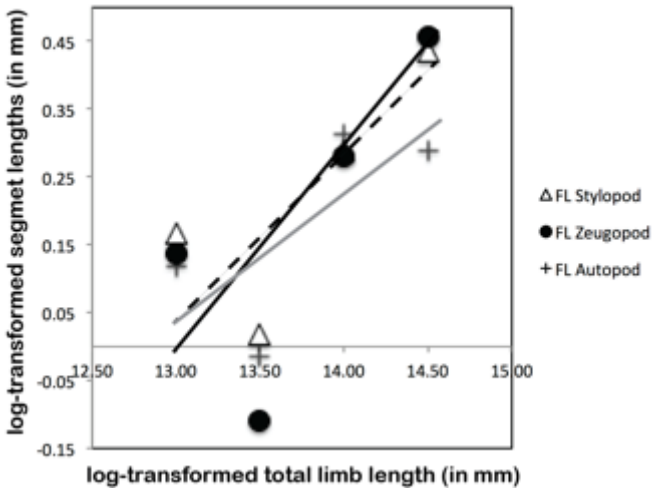

Figure 7. Adult segment proportions of both the fore- and hind limb in *M. musculus*.

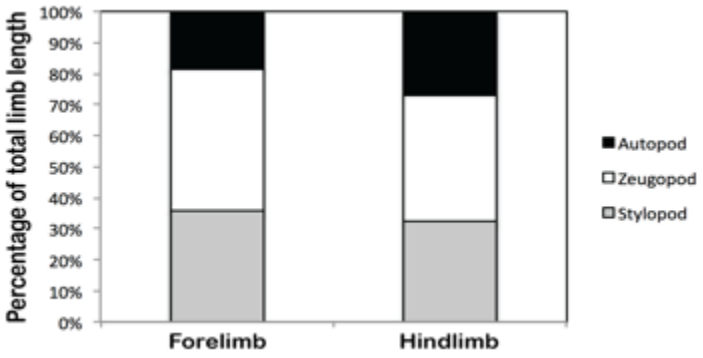

Figure 8. Divergence of fore- and hind limb segments throughout development.